DOI: 10.1002/ejoc.200900758

Mechanofluorochromism of a Series of Benzofuro[2,3-*c*]oxazolo[4,5-*a*]-carbazole-Type Fluorescent Dyes

Yousuke Ooyama,[a] Yusuke Kagawa,[a] Hiroshi Fukuoka,[a] Genta Ito,[a] and Yutaka Harima*[a]

Keywords: Mechanofluorochromism / Fluorescence / Dyes/pigments / Pi interactions / Amorphous solids

Mechanofluorochromism is found for a series of benzofuro[2,3-*c*]oxazolo[4,5-*a*]carbazole-type fluorophores (**1a**–**1d**) having cyano groups as acceptor: grinding of **1a**–**1d** induces a fluorescent color change with an enhanced quantum yield, and the fluorescent color is recovered by heating or exposure to solvent vapor. Interestingly, both absorption and emission peaks are redshifted by grinding, in conflict with the common view. On the basis of time-resolved fluorescence spectroscopy, X-ray powder diffraction (XRD), differential scanning calorimetry (DSC), and single-crystal X-ray structural analysis, the mechanofluorochromism observed with this new class of fluorescent dyes is found to accompany a reversible switching between crystalline and amorphous states with changes of molecular arrangement and intermolecular π–π interactions. An essential role of a strong donor-π-acceptor character of the dyes is pointed out for the manifestation of the observed mechanofluorochromism.

Introduction

The solid-state fluorescence of organic fluorescent dyes has recently attracted increasing interest both in the fundamental research field of solid-state photochemistry[1] and in the applied field of optoelectronic devices.[2] In particular, tunable solid-state fluorescence of organic dyes by application of an external stimulus is of great importance for developing optical recording devices and sensor systems.[3] Mechano- or piezofluorochromism found recently is a change in fluorescent color induced by mechanical stress, being accompanied with a reversion to the original fluorescent color by heating, recrystallization, or exposure to solvent vapor. It has been considered that the fluorescent color change is attributed to the interconversion between two different molecular aggregation states. Very recently, Araki et al. have reported the piezochromic luminescence of amide-substituted tetraphenylpyrene C6TPPy, composed of a planar fluorescent core and multiple hydrogen-binding sites, and explained it in terms of the change of intermolecular amide hydrogen bonds by grinding and heating.[4b] More recently, Sawamura et al. have found the mechanochromic luminescence of [$(C_6F_5Au)_2$(μ-1,4-diisocyanobenzene)]: grinding of the complex induced a photoluminescent color change, which was restored by exposure to a solvent. They have concluded that the intermolecular aurophilic interactions Au–Au presumably play a key role in the altered emission.[4d] At present, however, the number of organic dyes exhibiting mechanofluorochromism is still limited, and the mechanisms are not fully clarified.[4]

Here, we demonstrate that a series of donor-π-acceptor benzofuro[2,3-*c*]oxazolo[4,5-*a*]carbazole-type fluorophores (**1a**–**1d**) having cyano groups as acceptor display an obvious change in color and fluorescent color by pressing, and a reversion to the original colors by heating or exposure to solvent vapours (Figure 1). On the basis of time-resolved fluorescence spectroscopy, X-ray powder diffraction (XRD), differential scanning calorimetry (DSC), and single-crystal X-ray structural analysis, the mechanofluorochromism observed with this new class of fluorescent dyes is found to accompany a reversible switching between crystalline and amorphous states with changes of molecular arrangement and intermolecular π–π interactions, and an essential role of a strong donor-π-acceptor character of the dyes is pointed out for the manifestation of the observed mechanofluorochromism.

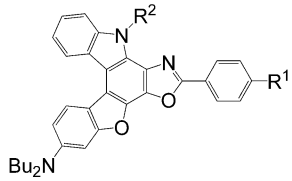

1a: R^1 = CN, R^2 = H
1b: R^1 = CN, R^2 = *n*-butyl
1c: R^1 = CN, R^2 = benzyl
1d: R^1 = CN, R^2 = 5-nonyl
1e: R^1 = *t*Bu, R^2 = H

Figure 1. Benzofuro[2,3-*c*]oxazolo[4,5-*a*]carbazole-type fluorophores **1a**–**1e**. Dye **1e** is synthesized for comparison purposes (see ref.[5] for **1a**–**1d** and Supporting Information for **1e**).

[a] Department of Applied Chemistry, Graduate School of Engineering, Hiroshima University
Higashi-Hiroshima 739-8527, Japan
Fax: +81-82-424-5494
E-mail: harima@mls.ias.hiroshima-u.ac.jp

Supporting information for this article is available on the WWW under http://dx.doi.org/10.1002/ejoc.200900758.

Results and Discussion

In 1,4-dioxane, the fluorophores **1a**–**1d** exhibit intense absorption bands at around 430 and 350 nm and a single intense fluorescence band at around 540 nm. The fluorescence quantum yields of **1a**–**1d** are almost 100%.[5] Time-resolved fluorescence spectroscopy of **1a**–**1d** indicated that the decay profile fitted satisfactorily a single exponential function (τ = 3.7–4.2 ns for **1a**–**1d**; see Supporting Information). The fluorophores **1a**–**1c** and **1d** when recrystallized from acetone were yellow and yellowish-orange, respectively, and all of them exhibited green fluorescence. The fluorescence excitation and emission maxima (λ_{max}^{ex} and λ_{max}^{em}) of **1a**–**1d** in the crystalline state were redshifted by 60–90 nm and 5–20 nm (compared with those for the corresponding dyes in 1,4-dioxane), respectively, and accompanied by a considerable decrease in the fluorescence quantum yield (Φ_F) (Table 1). The redshifts of λ_{max}^{ex} and λ_{max}^{em}, and the decrease of Φ_F by changing from solution to the crystalline state are quite common and explained in terms of π–π interactions in the crystalline state leading to delocalization of excitons or eximers.[3f,3g,4c,6,7]

Table 1. Solid-state photophysical data for **1a**–**1e** before and after grinding.

Compound	Excitation λ_{max}^{ex} [nm]	Emission λ_{max}^{em} [nm]	Φ_F[a]	τ_1 [ns][b,d] (A_1 [%])[c]	τ_2 [ns][b,d] (A_2 [%])[c]
1a (before)	507	561	<0.02	0.6 (77)	3.2 (23)
1a (after)	561	614	0.06	0.9 (37)	4.0 (63)
1b (before)	493	536	0.08	0.7 (75)	2.2 (25)
1b (after)	540	589	0.25	1.0 (18)	5.5 (82)
1c (before)	508	546	0.15	1.1 (46)	3.7 (54)
1c (after)	544	593	0.34	1.1 (15)	5.9 (85)
1d (before)	523	567	0.12	1.3 (22)	4.8 (78)
1d (after)	544	592	0.38	1.0 (14)	5.2 (86)
1e (before)	443	471	0.05	0.3 (96)	1.6 (4)
1e (after)	443	474	0.09	0.3 (83)	1.8 (17)

[a] Fluorescence quantum yield. [b] Fluorescence lifetime. [c] Fractional contribution. [d] The wavelength range of the time-resolved emission measurements were the range from λ_{max}^{em} to 65 nm at the shorter wavelength and the longer wavelength.

By grinding the solids in a mortar with a pestle, the dyes **1a**–**1d** changed their colors to orange and exhibited strong reddish-orange fluorescence. The photophysical data of **1a**–**1d** before and after grinding of as-recrystallized dyes are summarized in Table 1, together with those of **1e**. After grinding, the λ_{max}^{ex} and λ_{max}^{em} values for **1a**–**1d** are redshifted by 21–54 nm and 25–53 nm, respectively. The degrees of the redshift ($\Delta\lambda_{max}^{ex}$, $\Delta\lambda_{max}^{em}$) decrease in the order of **1a** (54, 53) > **1b** (47, 53) > **1c** (36, 47) > **1d** (21, 25), in agreement with the order of increasing steric sizes of the substituents. It is worth noting here that the Φ_F values increased by grinding from 0.02, 0.08, 0.15, and 0.12 to 0.06, 0.25, 0.34, and 0.38 for **1a**, **1b**, **1c**, and **1d**, respectively. When the ground samples were heated at 80–150 °C [over recrystallization (T_c), described later] or exposed to organic solvents such as acetone for several minutes, the dyes (except **1c**) recovered to the original colors. More rapid changes were observed for the cast film than the powder form, when the cast film on glass substrate was pressed with a spatula and then heated (5 s, 80 °C). The typical color and fluorescent color changes for powders of **1b** by grinding and heating are shown in Figure 2, together with the fluorescent color changes of its cast film. The reversibility of the color and fluorescent color is dependent on the substituents, and the dye **1d** with a bulky 5-nonyl substituent exhibited almost perfect color and fluorescent color changes (Figure 3 and Supporting Information). In contrast to the dyes **1a**–**1d**, the fluorescent dye **1e** did not exhibit appreciable changes of λ_{max}^{ex} and λ_{max}^{em} by grinding, although a slight increase of Φ_F was observed. The dye **1e** where the CN group is replaced by a *t*Bu group of less accepting character may be of less polar nature than the dyes **1a**–**1d**.

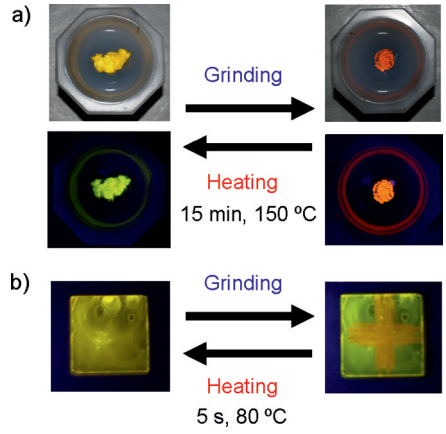

Figure 2. Photographs of (a) powder of **1b** under room light (top) and under UV irradiation (bottom), and of (b) cast film of **1b** under UV irradiation before and after grinding, and after heating the ground solid.

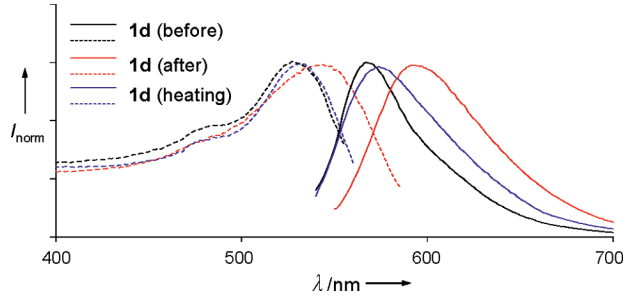

Figure 3. Excitation (dotted line) and fluorescence (solid line) spectra of **1d** before and after grinding, and after heating the ground solid at 150 °C.

Time-resolved fluorescence spectroscopy with the dyes **1a**–**1d** before and after grinding revealed that the fluorescence decay profiles, irrespective of grinding, fitted biexponential curves with fluorescence lifetimes of τ_1 = 0.6–1.3 ns and τ_2 = 2.2–5.9 ns, indicating the presence of two distinct emitting states. In case of **1a**, the emission wavelengths in the time-resolved measurements (λ_{max}^{trs}) were de-

pendent on the time window: for the as-recrystallized dye, 559 nm for 0–5 ns to 587 nm for 7–20 ns; for the ground dye, 614 nm for 0–5 ns and 620 nm for 7–20 ns. For the respective dyes (except **1a**), however, the λ_{max}^{trs} value was independent of the time window and coincided with the emission wavelength λ_{max}^{em} in normal fluorescence spectroscopy. The ratios of fractional contributions (A_1/A_2) decreased by grinding: $(A_1/A_2)_{after}/(A_1/A_2)_{before}$ = 0.18, 0.07, 0.21, and 0.57 for **1a**–**1d**, respectively. This appears to suggest that the A_1 and A_2 components correspond, respectively, to emissions from dye molecules in the mixed phase of crystalline and amorphous states, although this assignment proves to be incorrect by the X-ray measurements as described later.

The XRD measurements with as-recrystallized dyes **1a**–**1e** exhibited diffraction peaks ascribable to well-defined microcrystalline structures. After grinding, they almost disappeared, showing that the crystal lattice was significantly disrupted by grinding. As to **1d**, the diffraction peaks completely disappeared, although the decrease of A_1/A_2 by grinding was the smallest among the dyes **1a**–**1d**. This implies that the two emission components are highly unlikely to be assigned simply to dye molecules in crystalline and amorphous states. The values of λ_{max}^{trs} independent of the time window for most of the dyes support this conclusion. Except **1c**, the diffraction peaks of the ground dyes after being heated were quite similar to those before grinding, suggestive of recovery of the microcrystalline structure by heating.

A DSC analysis was carried out to clarify the thermal properties of these dyes. The results indicated that the dyes (except **1c**) before grinding showed only one sharp endothermic peak associated with melting. On the other hand, the ground solids underwent an endothermic glass transition (T_g) and then recrystallization (T_c) before melting (T_m). The XRD patterns and DSC curves for **1b** are shown in Figure 4. The DSC trace of the ground powder is typical of amorphous solids.[8] In contrast, the DSC trace of the crystal **1c** is typical of a polymorphic mixture; the dye before grinding showed a melting at 253.5 °C and then recrystallization of a stable modification at 258.1 °C, which in turn melts at 270.0 °C. The DSC data for **1a**–**1e** before and after grinding of as-recrystallized dyes are summarized in Table 2. The XRD and DSC studies suggest strongly that the mechanofluorochromism of **1a**–**1d** is not just a matter of events originating from a reversible change between crystalline and amorphous states by grinding and heating, because the dye **1e** did not exhibit such a mechanofluorochromism.

The dyes **1a**–**1d** have fairly large π-conjugated planes with electron-accepting and -donating moieties on both ends of the molecules. Because of this, they are expected to have large dipole moments in their ground states. Dipole moments of **1a**–**1e** were evaluated from semi-empirical molecular orbital (MO) calculations by the INDO/S method after geometrical optimizations by the MOPAC/AM1 method. The numerical values of **1a**–**1d** in the ground state are 5.13–5.21 D, much larger than 1.65 D for **1e**. When the

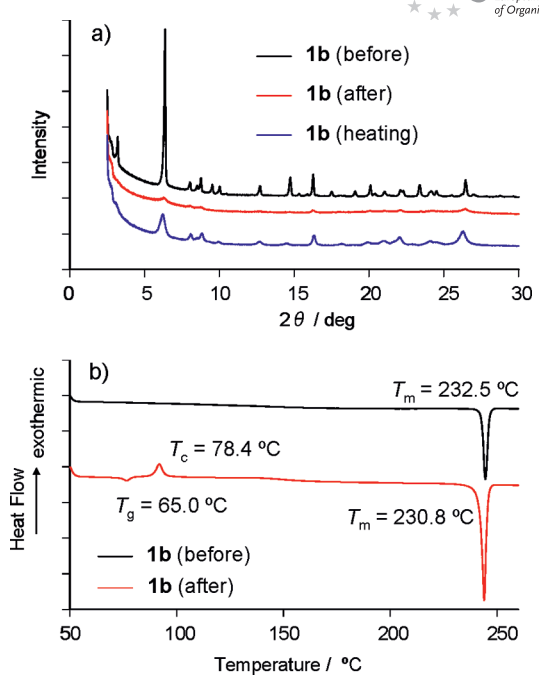

Figure 4. (a) XRD patterns and (b) DSC curves (scan rate: 10 °C min^{-1}) of **1b** before and after grinding, and after heating the ground solid.

Table 2. DSC data for **1a**–**1e** before and after grinding.

Compound	T_g [°C][a]	T_{crys} [°C][b] (ΔH [kJ mol^{-1}])	T_m [°C][c] (ΔH [kJ mol^{-1}])
1a (before)	–	–	295.5 (50.6)
1a (after)	102.1	122.8 (3.9)	291.6 (50.2)
1b (before)	–	–	232.5 (45.4)
1b (after)	65.0	78.4 (6.4)	230.8 (42.7)
1c (before)	–	258.1 (10.0)	253.5 (47.6), 270.0 (10.9)
1c (after)	87.7	117.2 (12.7)	271.7 (44.9)
1d (before)	–	–	192.7 (29.2)
1d (after)	66.7	92.9 (8.2)	187.4 (27.6)
1e (before)	–	–	232.9 (38.4)
1e (after)	104.6	134.5 (4.3)	231.5 (31.5)

[a] Glass transition temperature. [b] Crystallization temperature. [c] Melting point.

dyes are in the solid state, π–π interactions between adjacent molecular planes give rise to stacking of the dye molecules, therefore, the stacks will be arranged so as to minimize the dipole–dipole interactions. A single-crystal X-ray structural analysis was successfully performed only for **1d** (Figure 5a). The result indicates that the overlapping between π-planes of the fluorescent molecules is small owing to steric hindrance by the bulky 5-nonyl substituents. We see here two kinds of π-stacking arrangements, as shown by red and blue circles in Figure 5. The two stacking arrangements might be associated with the presence of two emitting states with different lifetimes, at least, for **1d**. The FT-IR study carried out with **1a** revealed that the absorption band at 3427 cm^{-1} ascribable to N–H stretching was broadened by grinding, although no appreciable changes in FT-IR spectra were observed for the rest of the dyes. The broadening of the absorption band may suggest the formation of

hydrogen bonds between the dye molecules. This may generate a new aggregation form in the amorphous phase, which is responsible for the two emission bands observed only for **1a**.

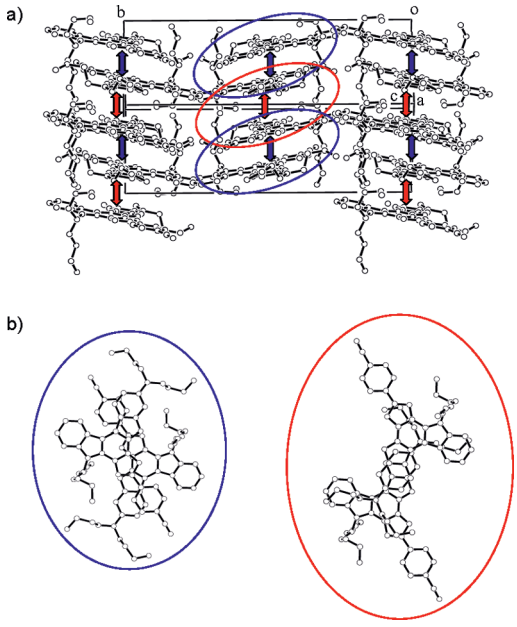

Figure 5. Crystal packing of **1d**: (a) stereoview of the molecular packing structure and (b) top view of the pairs of fluorophores. The red and blue up-down arrows represent the intermolecular π–π interactions. The red and blue circles show the π-staking arrangements.

In some pigments, the color tone of a pigment powder depends on the size of the particles. The different color tone is ascribed to the difference in the degree of light scattering on the pigment surfaces, so that the absorption background changes, but no appreciable shift of absorption peaks was observed. In the present experiments with the fluorescent dyes **1a**–**1d**, however, grinding of their powders induced shifts in peak wavelength of fluorescence spectra as well as absorption spectra. These spectroscopic observations rule out the possibility that the change in particle size is responsible for the color and fluorescent color changes observed with **1a**–**1d**. Moreover, the XRD and DSC measurements demonstrate that **1a**–**1d** interconvert between microcrystalline and amorphous states by grinding and heating. This suggests that the mechanofluorochromism of **1a**–**1d** is ascribable to a reversible change of molecular arrangement and intermolecular π–π interactions by grinding and heating. However, it is generally understood that intermolecular π–π interactions lead to a redshift of λ_{max}^{em} and a decrease of Φ_F because of a delocalization of excitons. Interestingly, the fluorescent dyes **1a**–**1d** in the amorphous states exhibit higher λ_{max}^{em} and Φ_F values than those in crystalline states, in conflict with the common view. One plausible explanation for the redshift of λ_{max}^{em} by grinding is that the amorphous states of the dyes **1a**–**1d** are such as allowing fluorophores to get closer so as to enhance π–π interactions between the highly polar dye molecules, as shown in Figure 6. It is worth noting here that the resulting interaction does not decrease the Φ_F value, but rather increase it by three times for **1a**–**1d**. In view of no appreciable changes in τ_1 before and after grinding for the respective dyes, this may suggest that a non-radiative decay route for the excited states is relatively discouraged by the π–π interactions in the amorphous states for this series of dyes. A full understanding of the mechanofluorochromism observed with **1a**–**1d** would thus appear to require further investigation, although there seems little doubt that the reversible color changes arise from a switching between crystalline and amorphous states of the dye molecules with large permanent dipoles, being accompanied by changes of molecular arrangement and intermolecular π–π interactions.

Conclusions

We have found a new class of donor-π-acceptor-type fluorescent dyes displaying mechanofluorochromism; this new class of fluorescent dyes accompanies a reversible switching between crystalline and amorphous states with changes of molecular arrangement and intermolecular π–π interactions. Their mechanofluorochromic properties are significantly dependent on the steric factor of the substituents,

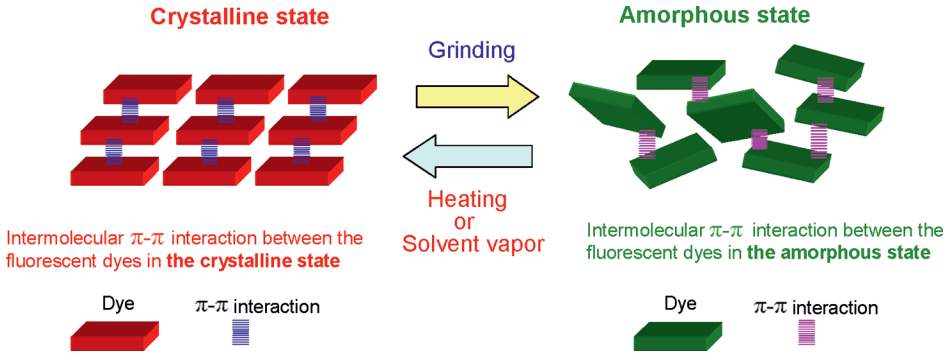

Figure 6. Mechanofluorochromism observed with **1a**–**1d**.

suggesting that the color and fluorescent color changes can be controlled by tuning the substitent group. We believe that these mechanofluorochromic fluorescent dyes can be a promising class of organic dyes for rewritable photoimaging and electroluminescence devices.

Experimental Section

General Information: Absorption spectra were recorded with a Shimadzu UV-3150 spectrophotometer, and fluorescence spectra were measured with a Hitachi F-4500 spectrophotometer. The fluorescence quantum yields (Φ) were determined by a Hamamatsu C9920-01 instrument equipped with CCD by using a calibrated integrating sphere system (λ_{ex} = 325 nm). Fluorescence lifetimes were determined with a Hamamatsu Photonics C4334/C8898 time-resolved spectrophotometer by excitation at 375 nm (laser diode). Powder X-ray diffraction measurements were performed with a Buruker D8 diffractometer with Cu-K_α radiator. Differential scanning calorimetry (DSC) of the samples was carried out by using a Shimadzu DSC-60 instrument.

X-ray Crystallographic Study: Crystals of **1d** were recrystallized from acetone as yellowish-orange prisms; they are air-stable. The one selected had approximate dimensions of $0.08 \times 0.12 \times 0.30$ mm. The data sets were collected at -100 ± 1 °C with a Rigaku RAXIS-RAPID Imaging Plate diffractometer by using graphite-monochromated Mo-K_α (λ = 0.71075 Å) radiation at 50 kV and 40 mA. In all cases, the data were corrected for Lorentz and polarization effects. All calculations were performed by using the teXsan[9] crystallographic software package of Molecular Structure Corporation. The transmission factors ranged from 0.72 to 1.00. The crystal structure was solved by direct methods using SIR92.[10] The structures were expanded by using Fourier techniques.[11] All non-hydrogen atoms were refined anisotropically. All hydrogen atoms were fixed geometrically and not refined. Crystal data: $C_{43}H_{48}O_2N_4$, M = 652.88, monoclinic, space group $P2_1/n$ (no. 14), a = 10.7160(7), b = 24.778(2), c = 13.694(1) Å, β = 98.201(2)°, V = 3598.8(5) Å^3, D_c = 1.205 g cm^{-3}, Z = 4, 32427 reflections measured, 8121 unique (R_{int} = 0.034). The final R indices were R_1 = 0.084, wR = 0.288 [$I > 2\sigma(I)$], GOF = 1.08. CCDC-681490 contains the supplementary crystallographic data for this paper. These data can be obtained free of charge from The Cambridge Crystallographic Data Centre via www.ccdc.cam.ac.uk/data_request/cif.

Computational Methods: The semi-empirical calculations were carried out with the WinMOPAC Ver. 3.9 package (Fujitsu, Chiba, Japan). Geometry calculations in the ground state were performed by using the AM1 method.[12] All geometries were completely optimized (keyword PRECISE) by the eigenvector following routine (keyword EF). Experimental absorption spectra of the eight compounds were compared with their absorption data by the semi-empirical method INDO/S (intermediate neglect of differential overlap/spectroscopic).[13–15] All INDO/S calculations were performed by using single-excitation full SCF/CI (self-consistent field/configuration interaction), which includes the configuration with one electron excited from any occupied orbital to any unoccupied orbital, where 225 configurations were considered [keyword CI (15 15)].

Supporting Information (see footnote on the first page of this article): Experimental details for photophysical data, DSC analysis, powder XRD, and crystallographic information.

Acknowledgments

This work was supported by Grants-in-Aid for Scientific Research (B) (19350094) from the Ministry of Education, Science, Sports and Culture of Japan, by Research for Promoting Technological Seeds from Japan Science and Technology Agency (JST), and by Furukawa Technology Promotion Foundation.

[1] a) Z. Fei, N. Kocher, C. J. Mohrschladt, H. Ihmels, D. Stalke, *Angew. Chem. Int. Ed.* **2003**, *42*, 783–787; b) Y. Sonoda, Y. Kawanishi, T. Ikeda, M. Goto, S. Hayashi, N. Tanigaki, K. Yase, *J. Phys. Chem. B* **2003**, *107*, 3376–3383; c) H. Langhals, O. Krotz, K. Polborn, P. Mayer, *Angew. Chem. Int. Ed.* **2005**, *44*, 2427–2428; d) A. Dreuw, J. Plötner, L. Lorenz, J. Wachtveitl, J. E. Djanhan, J. Brüning, T. Metz, M. Bolte, M. U. Schmidt, *Angew. Chem. Int. Ed.* **2005**, *44*, 7783–7786; e) Y. Kim, J. Bouffard, S. E. Kooi, T. M. Swager, *J. Am. Chem. Soc.* **2005**, *127*, 13726–13731; f) C.-H. Zhao, A. Wakamiya, Y. Inukai, S. Yamaguchi, *J. Am. Chem. Soc.* **2006**, *128*, 15934–15935; g) A. Wakamiya, K. Mori, S. Yamaguchi, *Angew. Chem. Int. Ed.* **2007**, *46*, 4273–4276.

[2] a) C. W. Tang, S. A. Vanslyke, *Appl. Phys. Lett.* **1987**, *51*, 913–915; b) L. S. Sapochak, F. E. Benincasa, R. S. Schofield, J. L. Baker, K. K. C. Riccio, D. Fogarty, H. Kohlmann, K. F. Ferris, P. E. Burrows, *J. Am. Chem. Soc.* **2002**, *124*, 6119–6125; c) C. J. Tonzola, M. M. Alam, W. K. Kaminsky, S. A. Jenekhe, *J. Am. Chem. Soc.* **2003**, *125*, 13548–13558.

[3] a) M. Irie, T. Fukaminato, T. Sasaki, N. Tamai, T. Kawai, *Nature* **2002**, *420*, 759–760; b) D. Xiao, L. Xi, W. Yang, H. Fu, Z. Shuai, Y. Fang, J. Yao, *J. Am. Chem. Soc.* **2003**, *125*, 6740–6745; c) R. Davis, N. P. Rath, S. Das, *Chem. Commun.* **2004**, 74–75; d) T. Mutai, H. Satou, K. Araki, *Nat. Mater.* **2005**, *4*, 685–687; e) Y. Mizobe, H. Ito, I. Hisaki, M. Miyata, Y. Hasegawa, N. Tohnai, *Chem. Commun.* **2006**, 2126–2128; f) R. Davis, N. S. Kumar, S. Abraham, C. H. Suresh, N. P. Rath, N. Tamaoki, S. Das, *J. Phys. Chem. C* **2008**, *112*, 2137–2146; g) N. S. S. Kumar, S. Varghese, N. P. Rath, S. Das, *J. Phys. Chem. C* **2008**, *112*, 8429–8437; h) Y. Sagara, T. Kato, *Angew. Chem. Int. Ed.* **2008**, *47*, 1–5.

[4] a) S. Mizukami, H. Houjou, K. Sugaya, E. Koyama, H. Tokuhisa, T. Sasaki, M. Kanesato, *Chem. Mater.* **2005**, *17*, 50–56; b) Y. Sagara, T. Mutai, I. Yoshikawa, K. Araki, *J. Am. Chem. Soc.* **2007**, *129*, 1520–1521; c) J. Kunzalman, M. Kinami, B. R. Crenshaw, J. D. Protasiewicz, C. Weder, *Adv. Mater.* **2008**, *20*, 119–122; d) H. Ito, T. Saito, N. Oshima, N. Kitamura, S. Ishizaka, Y. Hinatsu, M. Wakeshima, M. Kato, K. Tsuge, M. Sawamura, *J. Am. Chem. Soc.* **2008**, *130*, 10044–10045.

[5] a) Y. Ooyama, Y. Harima, *Chem. Lett.* **2006**, *35*, 902–903; b) Y. Ooyama, Y. Kagawa, Y. Harima, *Eur. J. Org. Chem.* **2007**, *22*, 3613–3621.

[6] a) H. Langhals, T. Potrawa, H. Nöth, G. Linti, *Angew. Chem. Int. Ed. Engl.* **1989**, *28*, 478–480; b) H.-C. Yeh, W.-C. Wu, Y.-S. Wen, D.-C. Dai, J.-K. Wang, C.-T. Chen, *J. Org. Chem.* **2004**, *69*, 6455–6462; c) Y. Ooyama, T. Okamoto, T. Yamaguchi, T. Suzuki, A. Hayashi, K. Yoshida, *Chem. Eur. J.* **2006**, *12*, 7827–7838.

[7] M. Kasha, in *Spectroscopy of the Excited State*, Plenum Press, New York, **1976**, pp. 337–363.

[8] a) S. Wang, W. K. Oldham Jr, R. A. Hudack Jr, G. C. Bazan, *J. Am. Chem. Soc.* **2000**, *122*, 5695–5709; b) H.-C. Yeh, R.-H. Lee, L.-H. Chan, T.-Y. J. Lin, C.-T. Chen, E. Balasubramaniam, Y.-T. Tao, *Chem. Mater.* **2001**, *13*, 2788–2796.

[9] *teXsan, Crystal Structure Analysis Package*, Molecular Structure Corporation, The Woodlands, TX, **1985** and **1992**.

[10] A. Altomare, M. C. Burla, M. Camalli, M. Cascarano, C. Giacovazzo, A. Guagliardi, G. Polidori, *J. Appl. Crystallogr.* **1994**, *27*, 435.

[11] P. T. Beurskens, G. Admiraal, G. Beurskens, W. P. Bosman, R. de Gelder, R. Israel, J. M. M. Smits, *The DIRIF94 Program System*, Technical Report of the Crystallography Laboratory, University of Nijmegen, The Netherlands, **1994**.
[12] M. J. S. Dewar, E. G. Zoebisch, E. F. Healy, J. J. Stewart, *J. Am. Chem. Soc.* **1985**, *107*, 3902–3909.
[13] J. E. Ridley, M. C. Zerner, *Theor. Chim. Acta* **1973**, *32*, 111–134.
[14] J. E. Ridley, M. C. Zerner, *Theor. Chim. Acta* **1976**, *42*, 223–236.
[15] A. D. Bacon, M. C. Zerner, *Theor. Chim. Acta* **1979**, *53*, 21–54.

Received: July 9, 2009
Published Online: August 27, 2009

